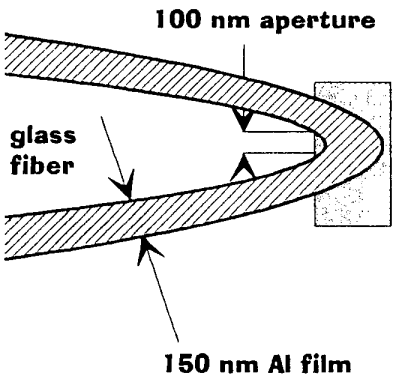

CTuC6 **Fig. 1.** Schematic diagram of the FIB milling procedure to produce a near-field aperture. The rectangular shaded region represents the area in which the ion beam raster scans over the tip from right to left in order to remove material cleanly.

result in redeposition of material onto the aperture, this procedure completely removes the material at the end of the fiber. By varying the size of the rectangular scanned region and with knowledge of the coating thickness and fiber end diameter, we can precisely make a clean-cut aperture of the desired diameter and optical throughput suitable for a variety of NSOM applications.

Figure 2 shows SEM images of the two apertures formed with the aforementioned FIB milling procedure with extremely well defined apertures of 100 nm diameter opening (a) and 300 nm diameter opening (b). The entire FIB milling time for each tip was between 2–3 minutes. As revealed in Fig. 2, the fabricated near-field apertures are, to the authors' best knowledge, the best defined and clean-cut ones ever fabricated. In contrast to angled metal evaporation, the FIB milling procedure removes any rough aluminum grains at the tip end surrounding the aperture. The advantages of this are twofold: the optical throughput is improved and the aperture can give the true near-field optical contrast of a sample without the influence of tip protrusions.

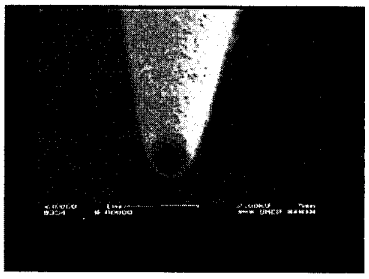

(a)

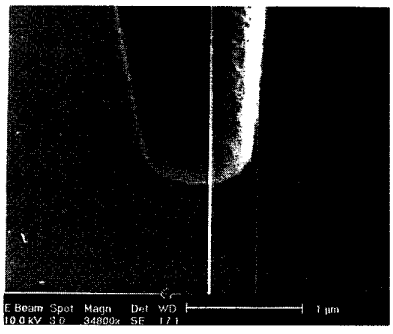

(b)

CTuC6 **Fig. 2.** SEM photographs of the near-field optical fiber probe (a) after FIB fabrication of a 100 nm diameter aperture (bar = 1 μm), and, (b) after FIB fabrication of a 300 nm diameter aperture (bar = 1 μm).

FIB fabricated fiber probes were tested in the near-field system developed in our laboratory.[3] The resolution obtained with these probes was of the order of the diameter of the fabricated aperture.

Institute for Plasma Research, University of Maryland, USA

***Present address: MIT Lincoln Labs, 244 Wood Street, Lexington, Massachusetts 02420-9108 USA*

1. D.W. Pohl, W. Denk, and M. Lanz, Appl. Phys. Lett. **44,** 651 (1984).
2. E. Betzig, J.K. Trautman, T.D. Harris, J.S. Weiner, and R.L. Kostelak, Science **251,** 1468 (1992).
3. W.A. Atia and C.C. Davis, Appl. Phys. Lett. **70,** 405 (1997).

CTuC7 9:30 am

Characterization of silicon micro-ring resonators using near-field scanning optical microscopy

G.H. Vander Rhodes, B.B. Goldberg, M.S. Ünlü, D.R. Lim,* K.K. Lee,* L.C. Kimerling,* *Departments of Physics and Electrical and Computer Engineering and the Photonics Center, Boston University, Boston, Massachusetts 02215 USA; E-mail: gregvr@bu.edu*

Micro-ring resonators have generated much interest in the optical telecommunications community for their use as high-Q, low-loss channel drop filters.[1] Many different variations in design and fabrication have been tested, including single and double ring designs, or disk types.[2] Far-field optical microscopy has been used for characterization of these devices, but no attempt has yet been made at imaging the standing mode field patterns inside the micro-ring.

Near-field scanning optical microscopy (NSOM) can image the optical emission and absorption properties of materials and devices at resolutions typically $< \lambda/10$. Near-field imaging relies on maintaining near-surface scanning and is thus ideally suited to collect evanescent optical fields which do not propagate into the far-field, and cannot be measured by conventional microscopy. We employ NSOM to map the internal optical modes of a micro-ring resonator.

A 0.5 μm × 0.2 μm single mode silicon strip waveguide is fabricated in a circular pattern to form a 4 μm radius ring to be used as a microcavity. A pair of waveguides placed close to the ring allow energy to be coupled in and out of the ring. This design is unique in that the input and output waveguides are placed over the ring in a high index contrast system. The advantage is that the lithography tolerances are relieved and standard UV lithography may be used to fabricate the rings. Furthermore, the Q of the ring can be tuned by varying the distance between the ring and the input and output waveguides. In our device the separation of the waveguide from the rings has been optimized to yield Q's of 5000.

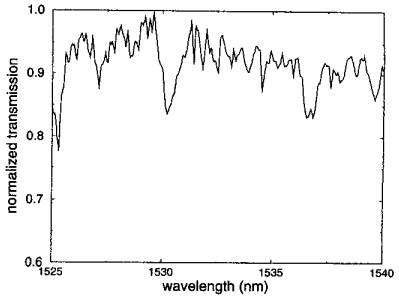

CTuC7 **Fig. 1.** Transmission spectra for the input waveguide of micro-ring resonator. Three resonance dips are clearly visible.

Transmission measurements of the source waveguide are displayed in Fig. 1. Three resonant drops in transmission are observed, though a calculation of extinction ratio yields a value of 0.3 dB, much lower than expected. At the resonant wavelength, there will be a drop in transmission because of the energy transfer to the other waveguide, but observation of the ring's output channel were unable to see any light exiting the structure. It is clear that the device as fabricated does not as expected.

We present data on new devices, recently fabricated.

**Department of Materials Science and Engineering, Massachusetts Institute of Technology, Cambridge, Massachusetts 02139; E-mail: drlcs@photonics.mit.edu*

1. K. Oda, S. Suzuki, H. Takahashi, and H. Toba, "An optical FDM distribution experiment using a high finesse waveguide-type double ring resonator," IEEE Photon. Technol. Lett. **6,** 1031–1034 (1994).
2. D. Rafizadeh, J.P. Zhang, S.C. Hagness, A. Taflove, K.A. Stair and S.T. Ho, "Waveguide-coupled AlGaAs/GaAs microcavity ring and disk resonantors with high finesse," Optics Letters, (1997).

CTuC8 9:45 am

Direct measurement of optical phase in the near-field

P.I. Phillips, J.C. Knight, P.St.J. Russell, G. Kakarantzas, J.M. Pottage, *Optoelectronics Group, Department of Physics, University of Bath, Claverton Down, Bath, BA2 7AY, United Kingdom; E-mail: pysplp@bath.ac.uk*

Traditionally, the most common measurement in optics is of electromagnetic field intensity. However, to fully characterise guided wave optical devices, one requires knowledge of the spatial variation of both the phase and amplitude within the device. In this work, we measure the intensity and relative phase in the